Spectrochimica Acta Part B xxx (2010) xxx–xxx

Contents lists available at ScienceDirect

Spectrochimica Acta Part B

journal homepage: www.elsevier.com/locate/sab

Femtosecond laser induced breakdown spectroscopy of silver within surrogate high temperature gas reactor fuel coated particles

D.E. Roberts [a,*], A. du Plessis [a,b], J. Steyn [a], L.R. Botha [a,b], C.A. Strydom [c], I.J. van Rooyen [d]

[a] CSIR National Laser Centre, PO Box 395, Meiring Naudé Road, Pretoria 0001, South Africa
[b] Laser Research Institute, Physics Department, University of Stellenbosch, Private Bag X1, Matieland 7602, South Africa
[c] Chemical Resource Beneficiation, North-West University, Private Bag X6001, Potchefstroom 2520, South Africa
[d] PBMR, Fuel Design, 1279 Mike Crawford Avenue, Centurion, 0046, South Africa

ARTICLE INFO

Article history:
Received 11 May 2010
Accepted 4 September 2010
Available online xxxx

Keywords:
Femto-LIBS
Silver
Zirconium oxide
Silicon carbide
Uranium dioxide
TRISO fuel coated particles

ABSTRACT

The detection of metallic silver on Chemical Vapour Deposited (CVD) grown silicon carbide and in Pebble Bed Modular Reactor (PBMR) supplied tri-structural isotropic (TRISO) coated particles (with 500 μm diameter zirconium oxide surrogate kernel) has been studied with femtosecond Laser Induced Breakdown Spectroscopy (femto-LIBS). The SiC layer of the TRISO coated particle is the main barrier to metallic and gaseous fission products of which ^{110m}Ag is of particular interest for direct cycle high temperature reactors. This work is a feasibility study for diagnosing and profiling silver transport through the silicon carbide layer of fuel particles for a high temperature gas reactor in out-of-reactor experimentation. The zirconium oxide is a surrogate for the enriched uranium oxide fuel. The conclusion reached in this study was that femto-LIBS can achieve good surface spatial resolution and good depth resolution for studies of silver in experimental coated particles. The LIBS technique also offers a good alternative for a remote analytical technique.

1. Introduction

The motivation for this study was the development of diagnostics for the profiling of silver through the SiC layer of the Pebble Bed Modular Reactor (PBMR) supplied tri-structural isotropic (TRISO) coated particles (CPs). The PBMR fuel (Fig. 1) consists of TRISO coated particles (CPs) (Fig. 1) in a graphite matrix. The three layer system, Inner Pyrolytic Carbon (IPyC)–Silicon Carbide (SiC)–Outer Pyrolytic Carbon (OPyC), forms the primary barrier to fission product release, with the SiC layer acting as the main pressure boundary of the particle [1,2]. This silicon carbide layer must prevent the transport of the radioactive products of the fission reactions as well as any gaseous products. The activation product, ^{110m}Ag, which is produced in the fission process in a reactor, can create a possible radiation hazard during maintenance of a direct cycle reactor. Plate-out occurs when the SiC layer fails to confine silver inside fuel coated particles and this leads to the entrainment of silver (Ag) in helium gas circulating through the reactor core [3,4]. The containment of silver inside the coated particles is a function of the temperature and SiC quality. The SiC layer must also have a high thermal conductivity to transport the fission-generated heat to the steam or helium gas used to drive the electrical generators.

Historically, some problems to manufacture the large number of fuel coated particles required for a reactor with a minimal fraction of failures of the SiC layer were identified. [5,6]. One particular problem associated with such coated particles has been the leakage of the radioactive silver isotope ^{110m}Ag [7,8], hence the use of silver in the present study. The percentage of coated particles that fail is relatively low (10^{-3}%, [8]) but should ideally be at least two orders of magnitude lower. The ^{110m}Ag transport mechanism in the intact SiC layer of TRISO coated particles has been studied for approximately 30 years without arriving at a satisfactory explanation for silver transport. It is still not clear why silver is preferentially lost from irradiated kernels though it appears it is not a straightforward diffusion mechanism [9]. PBMR has embarked on an experimental programme to study possible mechanisms in out-of-reactor research environment studies. Part of this experimental programme was to identify suitable analytical techniques for silver profiling.

Laser Induced Breakdown Spectroscopy (LIBS) offers advantages for such studies since it is a non-contact diagnostic method. Femtosecond LIBS (femto-LIBS) in particular offers additional advantages which are described in this paper. The present work is a feasibility study for femto-LIBS diagnostics, with the aim of producing depth profile information of silver leakage, with two main simplifications.

The first simplification is the use of PBMR supplied zirconium oxide (ZrO_2) coated particles (CPs) rather than enriched UO_2, though with the same dimensions. ZrO_2 has similar physical and thermal

* Corresponding author. Tel.: +27 12 841 4851; fax: +27 12 841 3152.
E-mail address: troberts@csir.co.za (D.E. Roberts).

0584-8547/$ – see front matter © 2010 Elsevier B.V. All rights reserved.
doi:10.1016/j.sab.2010.09.001

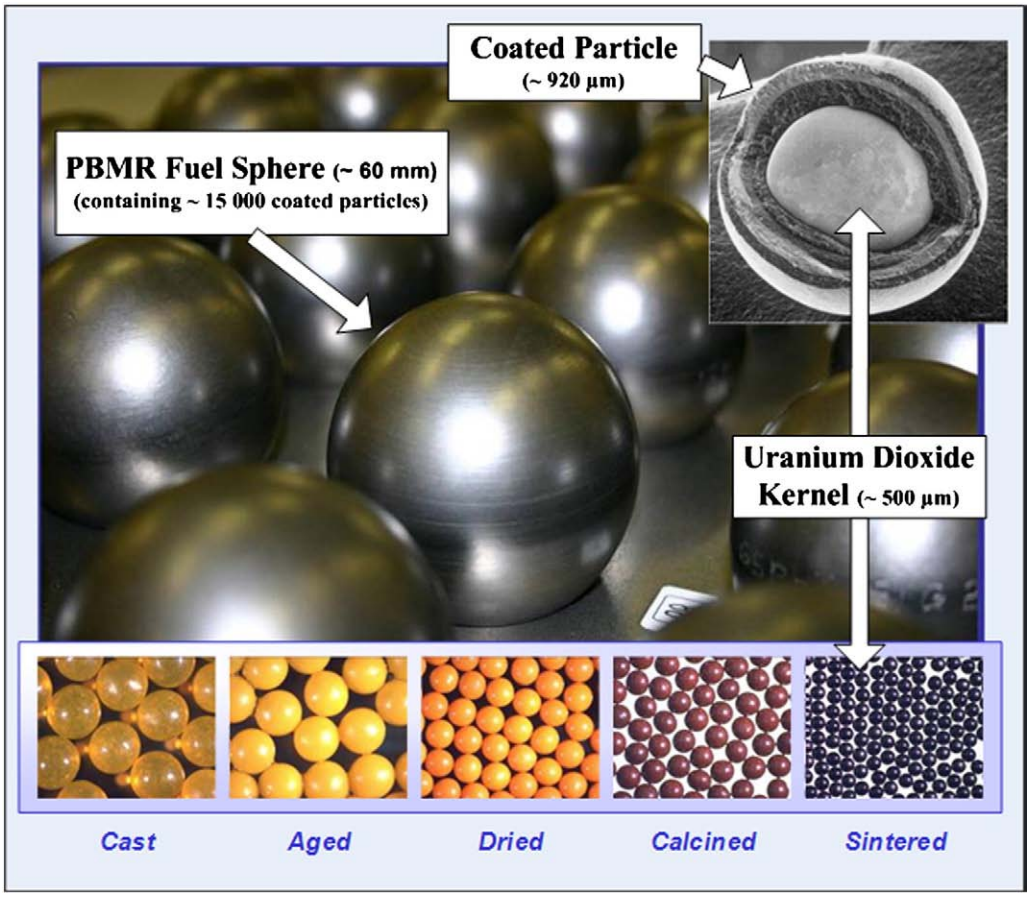

Fig. 1. PBMR fuel showing UO_2 fuel kernel and coated particle with CVD SiC coating.

properties to UO_2 [10,11] and is therefore often used as a "surrogate" to study problems associated with uranium fuel [12]. It has the advantage of being non-radioactive, making handling far easier. Enriched UO_2 is actually relatively harmless from the point of view of radioactivity [13] but is an alpha particle emitter and a chemically toxic substance. Therefore the generation of particles that can be transported through the atmosphere (as in LIBS), and can result in inhalation, must be avoided. After fission, UO_2 is very radioactive and further handling restrictions then apply.

The second simplification is the use of non-radioactive silver (containing the isotopes ^{107}Ag and ^{109}Ag). This is not a serious limitation, since neither the loss characteristic nor the spectral emission should depend on isotopic mass. The fraction of silver in the fission products of uranium [14] is relatively high (0.6%) so it is not critical that a very low limit of detection of silver is achieved. However, the complexity of the spectrum of uranium (>300,000 lines of U I in the visible and near UV [15]) and to a much lesser extent zirconium means that finding isolated spectral lines of silver for LIBS intensity measurements could be a challenge. Some of the difficulties of detecting impurities in bulk uranium and plutonium oxides have been reported in Ref. [16].

In the present work we focussed on laser parameters with the ultimate application in mind. For study purposes, radioactive fuel coated particles may be contained in thick-walled chambers under vacuum to exclude penetrating and airborne radiation losses. However, study of coated particles in a hot cell facility without a vacuum is also a possibility. In either case, there may not be close access to the fuel coated particles so the use of very short focal length lenses to focus the laser beam on the sample could be ruled out. Because of the relatively small size of the kernels (500 µm diameter), good surface spatial resolution is required (<25 µm). Good depth resolution is also required because the typical silicon carbide coatings are only 35 µm thick, while the transition region where silver could be trapped dictates a depth resolution of <1 µm. In addition, since we would like to detect silver as a function of depth in the CP, it is necessary to drill through most or all of the CP without having a hole of too low an aspect ratio. Finally, it would be highly desirable to minimise heat transport out of the ablation zone to avoid cracking the SiC layer or heating up of the fuel.

All these requirements point to the use of a femtosecond laser for LIBS. Sub-diffraction limited ablation means spatial resolutions of <20 µm can be achieved even with a relatively long focal length lens. Also depth resolutions of <1 µm are readily achievable, while the short pulses and low threshold for ablation mean virtually no heat-affected zone around the ablation area.

2. Experimental details

The experimental setup to view the LIBS plasma perpendicular to the sample is shown in Fig. 2. Two femtosecond laser systems were used in this study, with similar parameters. The first was a Coherent Legend regenerative amplifier system. The second was a Clark-MXR 2110 regenerative amplifier system. Both systems produce pulses at 1 kHz repetition rate with an average power of near 1 W, with durations of approximately 130 and 200 fs respectively. The Coherent Legend beam could be sent to a Michelson interferometer to generate double pulses with a separation of up to 3.4 ns [17].

The laser beam at the fundamental wavelength of the femtosecond laser (795 nm or 772 nm for the two systems respectively) was focused with a long focal length lens A (f = 300–500 mm) onto the sample C via a small elliptical mirror B with minor axis width of 10 mm. This led to minimal blocking of emitted radiation from the

Please cite this article as: D.E. Roberts, et al., Femtosecond laser induced breakdown spectroscopy of silver within surrogate high temperature gas reactor fuel coated particles, Spectrochim. Acta B (2010), doi:10.1016/j.sab.2010.09.001

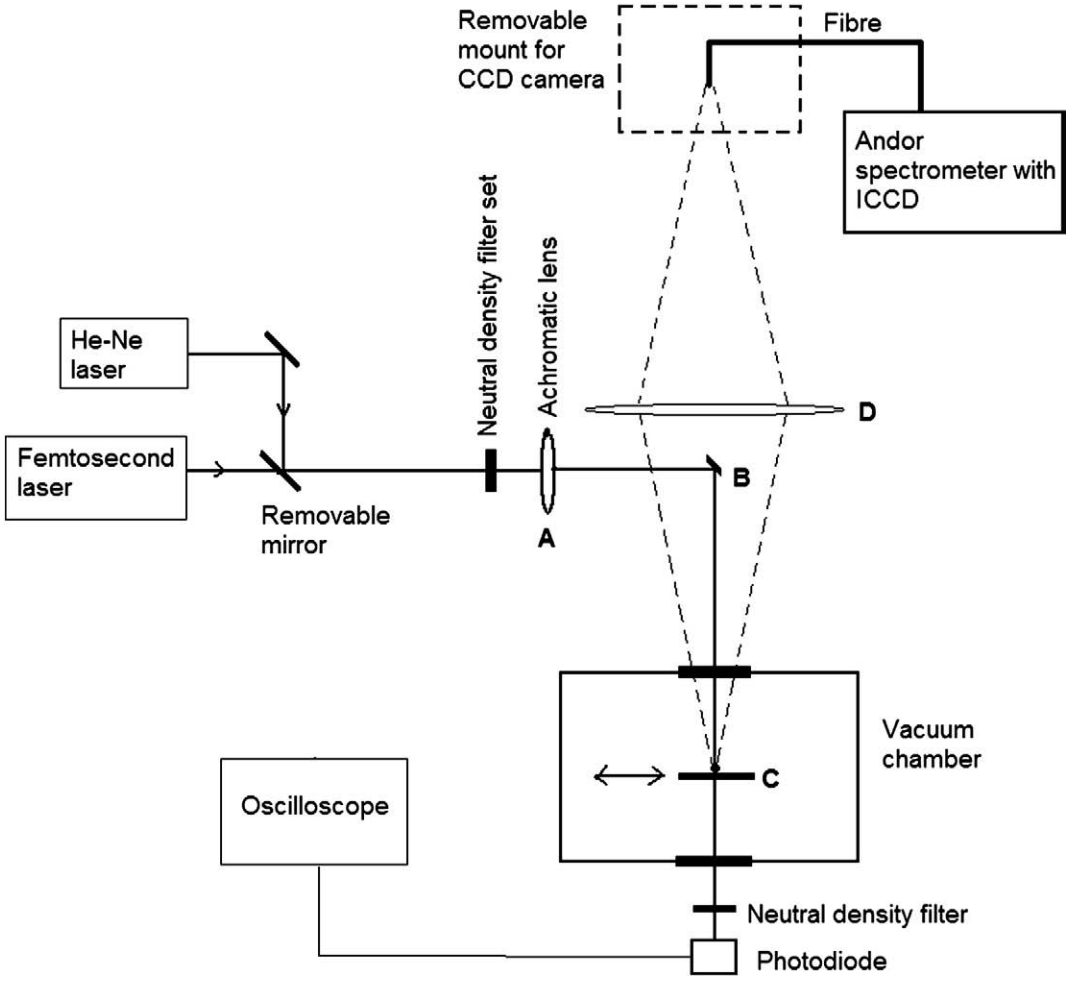

Fig. 2. Femto-LIBS setup for ablation of a ZrO_2 coated particle.

laser induced plasma at the sample, for collection by the large diameter (100 mm) lens D used to focus this light onto the fibre optic input of the spectrometer. The lens D was positioned so as not to restrict the solid angle of radiation from the back of the kernel.

The imaging spectrometer was an Andor Shamrock SR-303i with a turreted triple grating that can cover a wide wavelength range with different resolutions and is fitted with a DH734-18F-03 ICCD camera that enables spectra to be recorded for any pre-set delay time after the laser pulse with a minimum exposure (gate) time as low as 2 ns. The slit width was normally 50 μm with gratings with reciprocal dispersions of 10.7, 2.5 and 1.1 nm/mm resulting in wavelength resolutions of approximately 0.05–0.5 nm depending on the choice of grating. Wavelength calibration was done with a low pressure Hg-Ar lamp.

Some measurements were done with a Jarrel-Ash 82-410 spectrometer with a grating with reciprocal dispersion of 1.6 nm/mm (wavelength resolution of approximately 0.2 nm with 10 micron slit width) and a fast response time (1 ns rise time) high gain photomultiplier detector. This gave an excellent time resolution from each laser pulse but only the total intensity in one narrow band of the spectrum, corresponding to a single spectral line, could be recorded at a time.

The laser was normally operated in burst mode with the oscilloscope triggered at the start of the burst and the number of pulses needed to penetrate the sample obtained from the delay on the signal from a photodiode viewing the transmission from the rear of the sample (Fig. 2). There was zero time delay between the start of each pulse and the Jarrel-Ash recording. The fibre was mounted on a magnetic base and could be replaced by a camera for lining up with a He-Ne laser beam colinear with the femtosecond beam. The sample was on a precision x-y-z translation stage to optimise positioning of the beam on the sample.

Fuel CP experiments were done with the jig shown in Fig. 3. This was made from a 600 μm thick aluminium oxide plate in which a matrix of holes with a spacing of 1 mm was drilled with a Q-switched Nd:YAG micro-machining facility. To contain the CPs these holes were tapered, with an entrance diameter of 730 μm and exit diameter 560 μm for both ZrO_2 kernels and PBMR supplied coated particles. All spheres were fixed in position with epoxy glue.

A matrix of smaller holes of 250 μm entrance diameter and 160 μm exit diameter were drilled around these holes (Fig. 3) for alignment purposes. The signal on the photodiode used for kernel transmission measurements could be optimised on a small hole with the femtosecond beam at low power, such that no ablation occurs. After this alignment, the x-y-z stage then simply had to be moved by a multiple of 1 mm in one or two axes to position the beam on the centre of a sphere.

Three sets of experimental samples were prepared for this study:

- SiC layers were deposited on flat graphite samples using a chemical vapour deposition (CVD) method. A thin (20 μm) layer of silver paint (SPI conductive paint containing 43% silver solids) was also applied.
- Spherical ZrO_2 kernels, with a thin (20 μm) layer of silver paint applied to the front and back surfaces of the kernel to simulate leakage of silver from the interior.

Please cite this article as: D.E. Roberts, et al., Femtosecond laser induced breakdown spectroscopy of silver within surrogate high temperature gas reactor fuel coated particles, Spectrochim. Acta B (2010), doi:10.1016/j.sab.2010.09.001

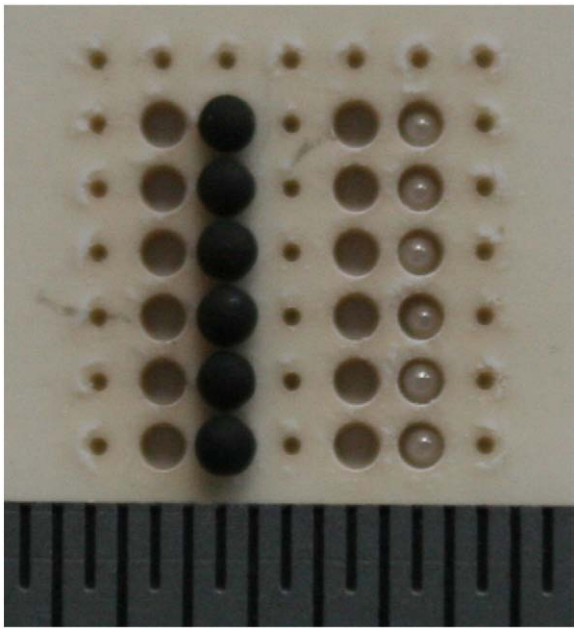

Fig. 3. Jig to contain surrogate fuel kernels showing a row of ZrO_2 kernels and a row of PBMR supplied coated particles complete with pyrocarbon and silicon carbide coatings. The smaller holes are for alignment. (The scale shows intervals of 0.5 and 1.0 mm).

- PBMR supplied experimental coated particles containing silver, also with a thin layer of silver paint applied to the front and back surfaces.

3. Results

The experiment was conducted in two parts. The first involved the detection of silver on the surface of silicon carbide to determine the sensitivity of depth profiling. The second was the detection of silver as a function of depth (a few 100 μm depth) in the PBMR experimental CPs containing silver.

Double femtosecond pulses with an appropriate pulse separation are known to lead to significant increases in line emission intensities and therefore signal to noise ratios [18–22]. For this reason, we initially used double femtosecond pulses as in Ref. [17]. However, subsequently it was found that low signal to noise ratios were not a concern so the LIBS measurements were moved to the Clark laser to make the Coherent system available for unrelated experiments.

The depth of substrate ablated per laser pulse in the femtosecond regime is primarily a function of pulse fluence [23,24]. The depth–fluence characteristics were therefore measured for the substrates of interest: silver paint and silver foil, CVD silicon carbide and ZrO_2.

The fluence was calculated from measurements of beam average power, P, pulse repetition rate, f_R, and focal length, f, of the lens imaging on the target. It was found from measurements of the power transmission of apertures of different radii that the pulse fluence profile, F(r), was a good approximation to a Gaussian distribution:

$$F(r) = F_0 \exp\left(-\frac{2r^2}{\omega^2}\right), \tag{1}$$

where ω was the waist radius at which the intensity fell to $1/e^2$ of its peak value at the focusing lens. From aperture measurements over a long distance of beam propagation (30 m) it was possible to estimate the beam quality factor [25] as:

$$M^2 = 1.3 \pm 0.2. \tag{2}$$

If the beam is focussed by a lens of focal length f to a waist radius ω_0' on the substrate then from [25]:

$$\omega_0' = \frac{M^2 \lambda f}{\pi \omega_0}. \tag{3}$$

The fluence on the beam axis can then be estimated from Eq. (3) and the relation:

$$F(0) = \frac{2E_t}{\pi \omega_0'^2}. \tag{4}$$

Here the pulse energy $E_t = P/f_R$.

Ultimately, it may be necessary to do some measurements in a vacuum to prevent airborne transport of radioactive materials. Therefore tests were done to find the difference in ablation efficiency in air and vacuum. Measurements of the ablation depth per pulse as a function of pulse fluence for 25 μm thick silver metal foil in air and vacuum are shown in Fig. 4(a). The ablation rate was about a factor of two lower in air than vacuum at a fluence of 40 Jcm^{-2} even though only 0.7% of the beam power was absorbed by the air plasma (Fig. 4(b)). At the transition fluence of 20 Jcm^{-2}, where air and vacuum efficiencies start to differ, the power absorbed by air breakdown was negligible (Fig. 4(b)) but the visible radiation from the beam fell off significantly here (Fig. 4(c)) suggesting that the reduction in ablation efficiency was due to the modification of the beam propagation characteristics rather than the reduction of pulse energy.

Measurements of the ablation depth per pulse as a function of pulse fluence are shown in Fig. 5 for silver foil, silver paint and SiC, all with planar samples. These are average depths, in the case of solid silver for drilling through 25 μm thick foil and in the other cases for drilling depths of from 20 μm to 100 μm as measured with a microscope with a calibrated depth of focus. For these flat surface studies, low fluences could be used for which there was little difference between vacuum and air ablation. Measurements on ZrO_2 CPs in air require higher fluences in order to drill through the whole sample (500 μm to 900 μm, depending on the coating). For fluences <10 Jcm^{-2} penetration could not be achieved no matter how many pulses were used.

Initial depth profiling measurements with SiC were made on planar samples coated on 3 mm square graphite substrates from a similar CVD coating facility used for the manufacturing of the CPs. An indication of the good surface spatial resolution achievable with the femto-LIBS setup is shown in Fig. 6 with the camera focussed on the surface (Fig. 6(a)) and below the surface (Fig. 6(b)).

Fast frame measurements of silver and silicon line intensities from CVD silicon carbide coated with silver paint are shown in Fig. 7. These records correspond to 10 successive laser pulses on the surface. For each pulse only the first 100 ns of the LIBS time sequence is shown and the bulk of the 1 ms between pulses, which is of no interest, is not recorded. The results in Fig. 7 were obtained with the Jarrell Ash spectrometer centred on a well-isolated Ag I line (328.07 nm, Fig. 7(a)) then on an isolated Si I line (288.16 nm, Fig. 7(b)) and show clearly the transition from the silver layer to the underlying silicon carbide substrate. Energy level diagrams for these and other lines used in the LIBS measurements are shown in Fig. 8.

Fig. 7(a) shows the first 10 laser shots ablating the surface. The first five pulses in Fig. 7(a) are mainly due to Ag I radiation while the sharp spikes in subsequent frames are from the short-lived continuum radiation after removal of the silver layer. The first pulse is significantly larger than the following pulses. This is due to the higher continuum intensity (but *not* silver line intensity after subtraction of the continuum) and is typical of ablation of a fresh surface where a thin layer of oxide and/or grease contamination is more easily ablated and yields a stronger continuum than the bulk material.

Please cite this article as: D.E. Roberts, et al., Femtosecond laser induced breakdown spectroscopy of silver within surrogate high temperature gas reactor fuel coated particles, Spectrochim. Acta B (2010), doi:10.1016/j.sab.2010.09.001

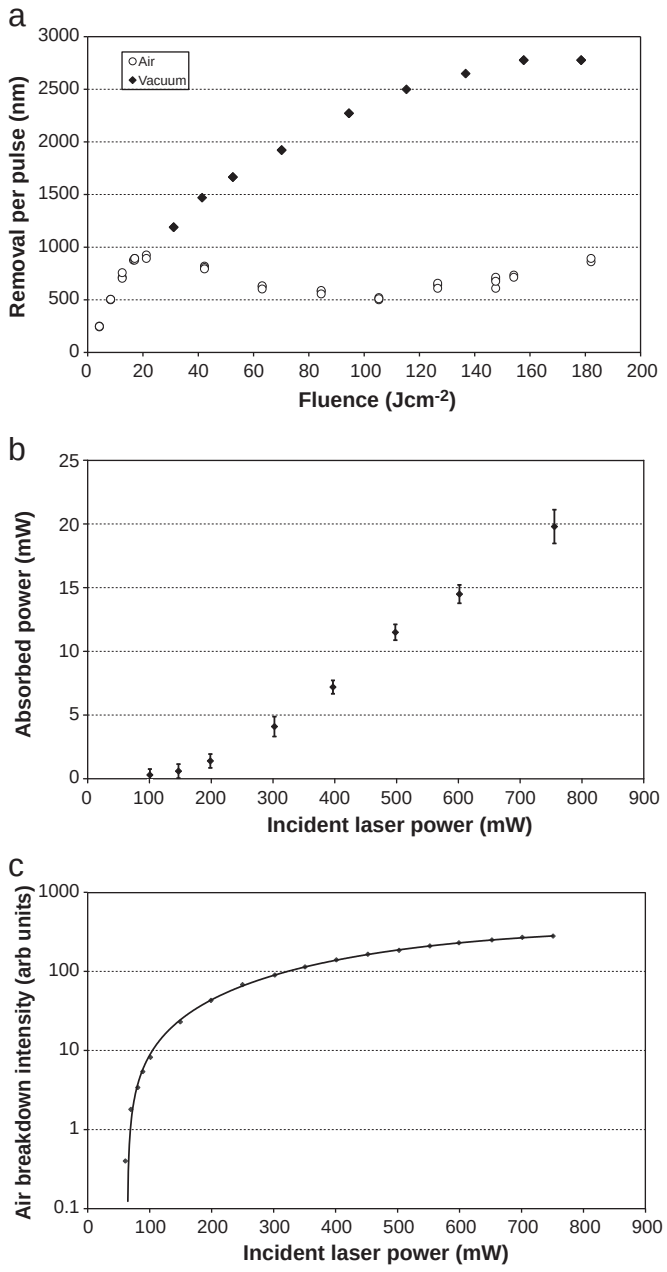

Fig. 4. (a) Removal rate per pulse for silver foil in air and vacuum (b) power absorbed by air breakdown plasma and (c) radiation from air plasma, for 150 fs pulse duration.

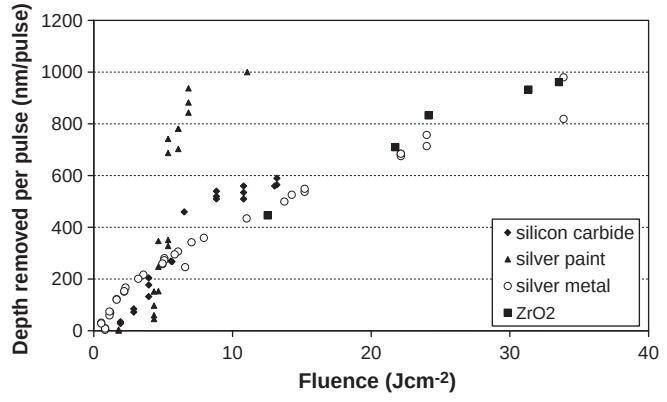

Fig. 5. Average ablation rate per pulse of Ag metal, Ag paint, SiC, and ZrO_2 in air as a function of fluence for 150 fs pulse duration.

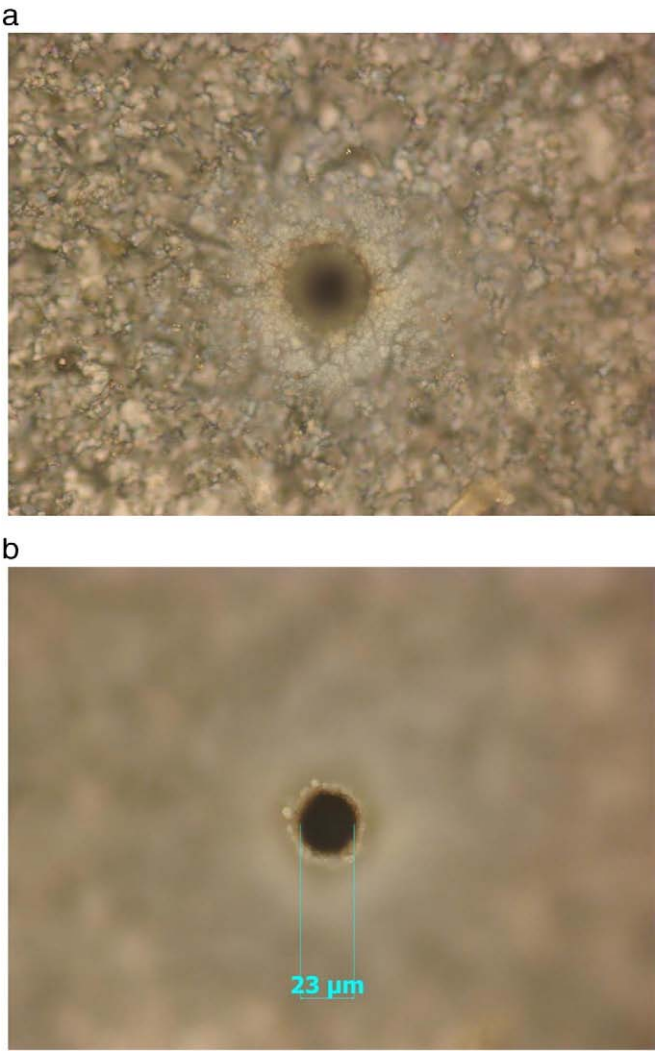

Fig. 6. Hole ablated in SiC sample with 512 pulses at 29 µJ/pulse. Focus on the surface (a) and below the surface (b).

The silicon line intensity is seen to appear on the 5th frame after "burn through" of most of the silver (Fig. 7(b)). It peaks at later times than the continuum intensity as seen clearly on subsequent frames. Peak relative intensities of silver and silicon lines from fast frame recordings are shown in Fig. 7(c) where, using the ablation-fluence characteristics of silver and silicon (Fig. 4), the time scale has been converted to a depth scale. Conversion of the intensity scale to an absolute density scale is discussed in the next section.

The depth resolution seen in Fig. 7(c) is about 1 µm. The smeared out transition for silver to silicon removal is mainly due to the Gaussian fluence profile. The depth resolution can be further improved by working at nearer to the ablation threshold. A significant improvement would be made with a "top hat" spatial distribution of fluence which is one of the aims of future work.

A typical LIBS recording with the Andor spectrometer showing the relative complexity of the spectrum from a ZrO_2 kernel is shown in Fig. 9. Lines of Zr II were particularly persistent so a delay of 200 ns with a gate width of 500 ns was used for recording spectra. The line and continuum intensity were fairly uniform up to about halfway through the kernel before falling off steadily to penetration (Fig. 10). Results of depth profiling right through a PBMR supplied experimental CP containing silver, with silver paint on the surface in addition, are shown in Fig. 11. Fig. 11(a) shows clearly the resonance lines of Ag I (328.07 nm, 338.29 nm, see Fig. 8) emitted from the surface (paint) layer. Fig. 11(b) shows Zr I and Zr II lines from the bulk of the CP after

Please cite this article as: D.E. Roberts, et al., Femtosecond laser induced breakdown spectroscopy of silver within surrogate high temperature gas reactor fuel coated particles, Spectrochim. Acta B (2010), doi:10.1016/j.sab.2010.09.001

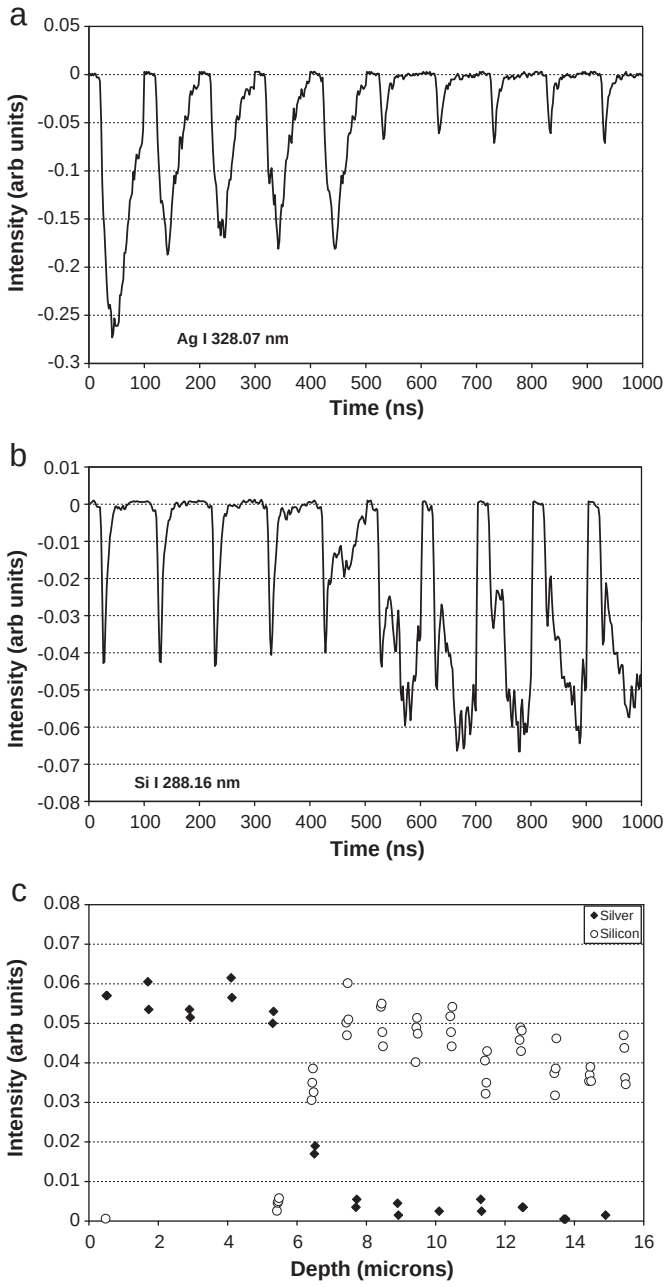

Fig. 7. Fast frame recordings of (a) Ag I line intensity (b) Si I line intensity and (c) interpretation in terms of depth profile.

penetration through the surface layer. The Ag I resonant line emission from the silver inside the CP is seen in Fig. 11(c). From depth profiling calculations, the position of this silver could be found to ±2 μm. The lines are very strongly broadened due to the large optical depth as well as exhibiting re-absorption at the centre of the lines due to plasma inhomogeneity. Finally, Fig. 11(d) shows the Ag I resonance lines from the surface layer at the back of the CP. These are seen in absorption in the continuum emission from the plasma.

4. Discussion

Here we consider the estimation of absolute densities of silver from line intensities in order to see the likely detection limits compared with minimum densities needed to be measured in future scenarios. It was necessary to use a calibration free technique [26,27] since measurements with ZrO_2 and ultimately uranium samples containing known amounts of impurities was not considered feasible. Since we are not concerned with measurements of trace elements within the *bulk* of the zirconium itself, problems with lack of stochiometry should not arise.

The density of silver atoms relative to the (known) density of silicon or zirconium atoms in the sample could be estimated from the relative intensity of a neutral silver line to a neutral silicon or zirconium line. If we assume local thermodynamic equilibrium (LTE) holds (discussed below) the relative density for zirconium is [27]:

$$\frac{n_{Ag}}{n_{Zr}} = \frac{I_{Ag}\lambda_{Ag}U_{Ag}(T_e)g_{Ag}A_{Ag}}{I_{Zr}\lambda_{Zr}U_{Zr}(T_e)g_{Zr}A_{Zr}}\exp\left(\frac{E_{Ag}-E_{Zr}}{kT_e}\right). \quad (5)$$

This assumes that the total particle densities consist of predominantly neutral species (see below). Here I is the intensity and λ the wavelength of a line with upper level energy E, statistical weight g and transition probability A. U is the partition function.

Strong and reasonably well-isolated lines chosen for the density ratio estimates were Ag I 338.29 nm, Zr I 360.12 nm and Si I 288.16 nm (Fig. 8). An advantage of the *Ag* I and *Zr* I lines is that they are fairly close in wavelength so knowledge of the relative response of the detection system is not critical. Calculated ratios n_{Ag}/n_{Zr} and n_{Ag}/n_{Si} as a function of electron temperature for unit line intensity ratios are shown in Fig. 12. Spectral line parameters were obtained from Refs. [28,29] and partition functions from Ref. [30]. For the *Ag* I and *Zr* I lines, $E_{Ag}-E_{Zr} = 0.068\ \text{eV} \ll kT_e$ so the exponential in Eq. (5) is a very weak function of T_e in the range of interest. However, due to the close packed energy level structures of the heavier atoms, the partition functions are strong functions of T_e. This means it is necessary to measure T_e to make reasonable estimates of the density ratios using Eq. (5) and Fig. 12.

The electron temperature was measured from the relative intensity of two spectral lines assuming LTE [31]:

$$\frac{I_A}{I_B} = \frac{\lambda_B g_A A_A}{\lambda_A g_B A_B}\exp\left(-\frac{\Delta E_{AB}}{kT_e}\right). \quad (6)$$

From Eq. (6), the percentage error in the estimate of T_e is the percentage error in measuring the intensity ratio multiplied by $kT_e/\Delta E$ so the larger ΔE_{AB} the better (except insofar as it is then more difficult to satisfy the LTE criterion, as seen below). Silver is a convenient element for the determination of T_e since the upper levels of the non-resonance doublet 520.91 nm and 546.55 nm and the resonance doublet 328.07 nm and 338.29 nm have a relatively large energy separation (Fig. 8). Specifically, for 546.55 nm and 338.29 nm, $\Delta E = 2.383$ eV (Fig. 8). The relative response of the system for these different wavelengths was measured with a tungsten-halogen quasi-continuous light source. We then found a spatial and time averaged $T_e = 0.85 \pm 0.1$ eV for the delay and detection window used.

For both density ratio and T_e measurements from Eqs. (5) and (6) it is implicitly assumed that the spectral lines used are optically thin [32]. The optical thinness of the lines studied could be readily checked from the relative intensity of the lines *within* each doublet.

If both lines A and B of a doublet are optically thick, their intensity ratio I_{Amax}/I_{Bmax} would approach unity, as seen with the lines in Fig. 11(d). This was, of course with solid silver. No attempt was made to analyse the strongly self-absorbed lines as in Fig. 11(c) as the densities expected in practical applications would be too low to cause such effects. In scenarios with surface coatings of silver where T_e and n_e were measured the densities were considerably less than solid values. In the case of optically thin lines, the ratio, assuming spatial homogeneity and LTE would be very close to the ratio of statistical weights of the upper levels. This is indeed approximately the case for the lines shown in Fig. 11(a).

Please cite this article as: D.E. Roberts, et al., Femtosecond laser induced breakdown spectroscopy of silver within surrogate high temperature gas reactor fuel coated particles, Spectrochim. Acta B (2010), doi:10.1016/j.sab.2010.09.001

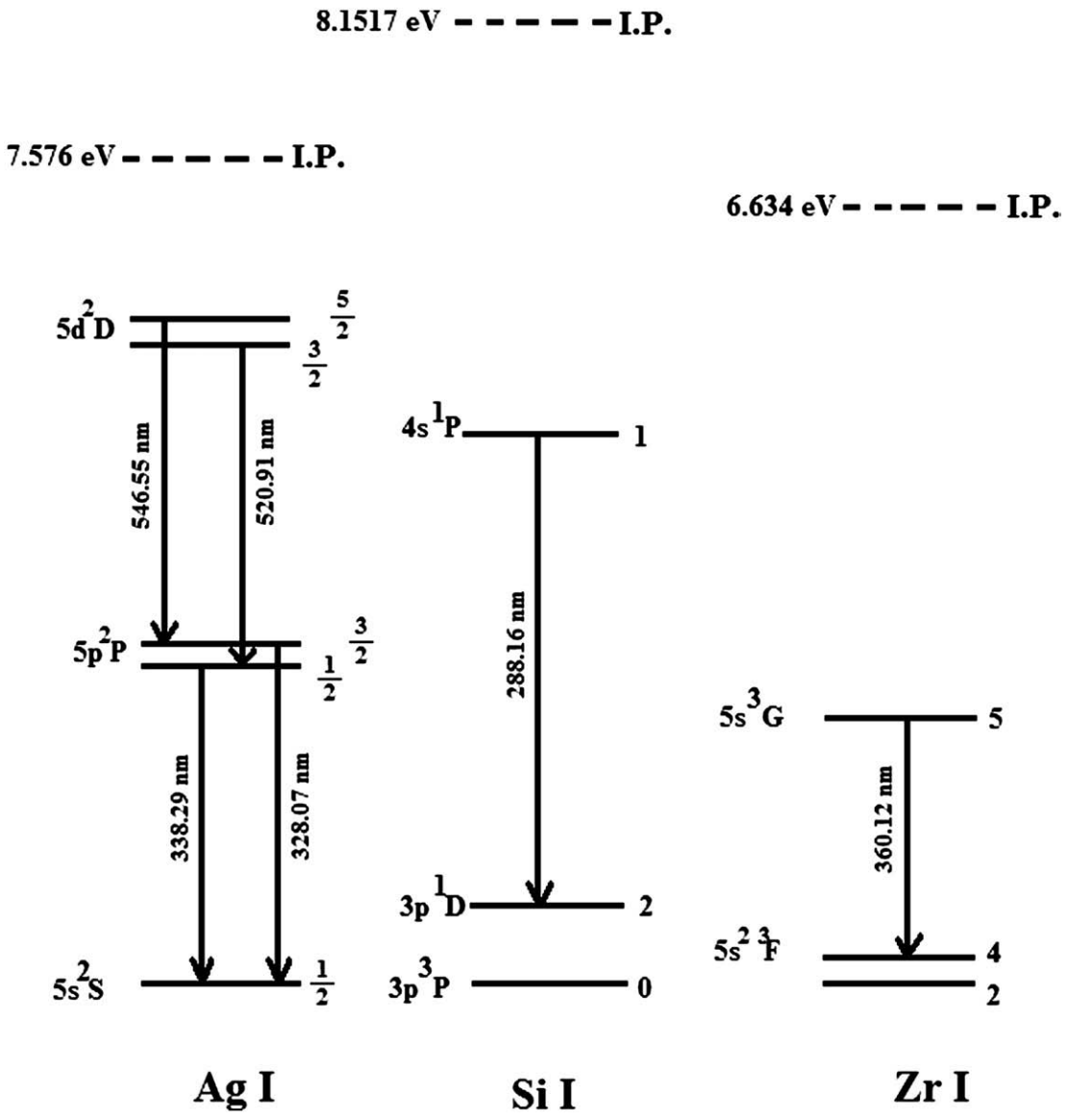

Fig. 8. Neutral silver, silicon and zirconium transitions used in the present work.

To investigate the assumption of LTE a necessary (though not sufficient [33]) condition for LTE given by McWhirter [34] was used.

$$n_e > 1.6 \times 10^{18} T_e^{1/2} (\Delta E)^3 m^{-3} \quad (7)$$

Here T_e is in K and ΔE in eV. The RHS of relation (6) does not depend too sensitively on T_e so T_e derived from relation (6) which assumes LTE for use in criterion (7) to justify LTE is not too critical. ΔE is the energy gap for which electron collisions populate an upper state.

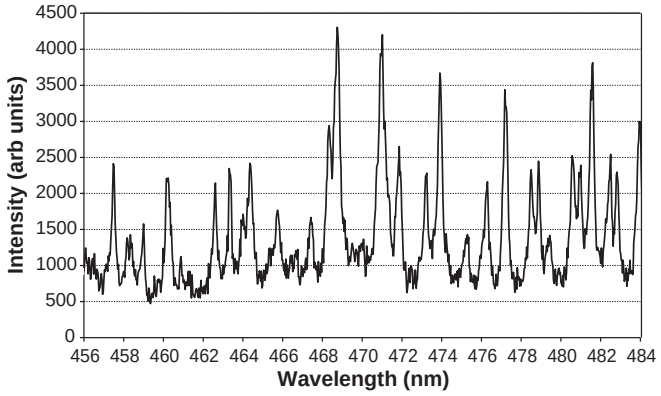

Fig. 9. LIBS spectrum of Zirconium from a coated particle for the wavelength range from 456 nm to 484 nm.

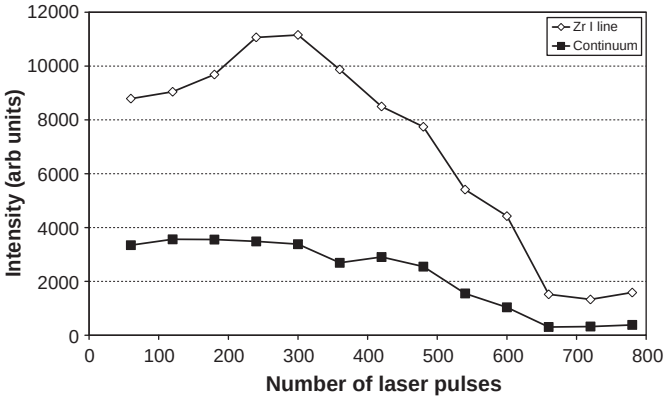

Fig. 10. Intensity of Zr I line and continuum from zirconium dioxide coated particle as a function of number of laser pulses. Penetration of coated particle occurs after 660 pulses.

Please cite this article as: D.E. Roberts, et al., Femtosecond laser induced breakdown spectroscopy of silver within surrogate high temperature gas reactor fuel coated particles, Spectrochim. Acta B (2010), doi:10.1016/j.sab.2010.09.001

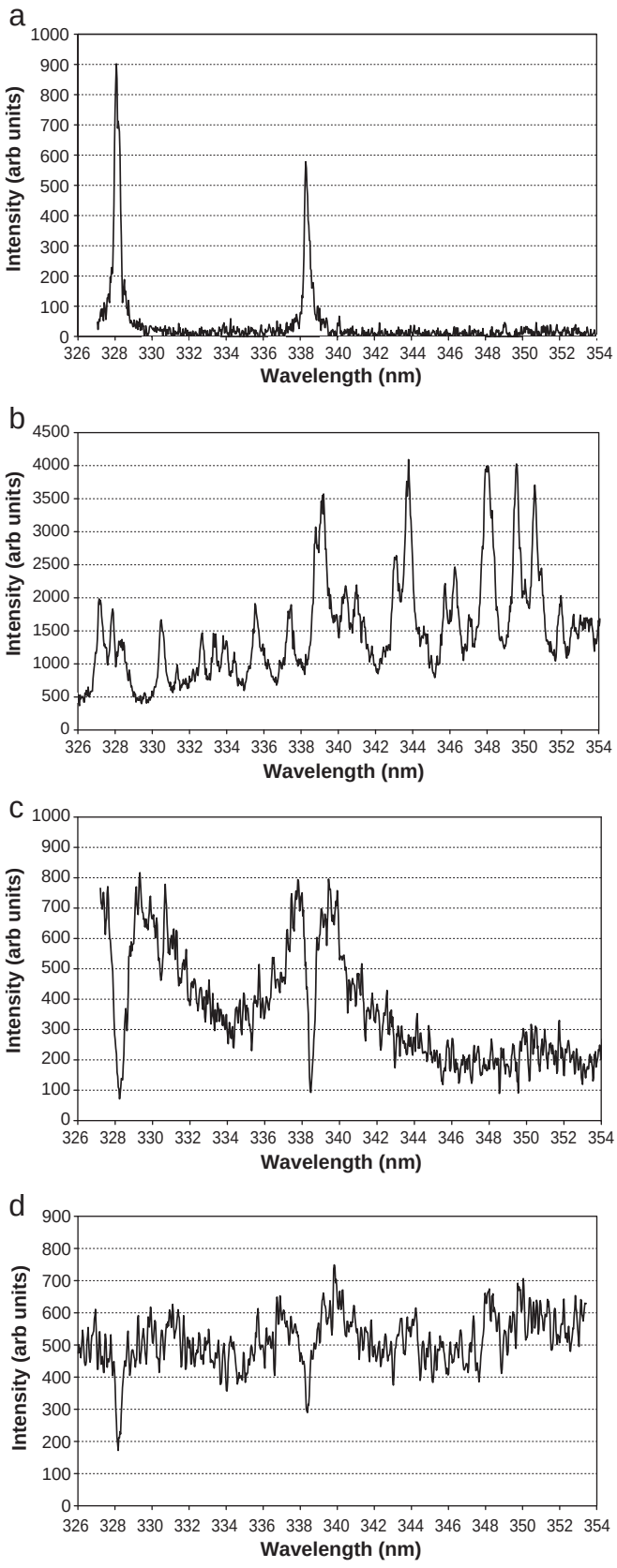

Fig. 11. Twenty-eight nm spectral region at different depths of coated particle with silver surface paint layer and silver in the PBMR supplied coated particle. (a) Ag resonance lines at front surface. (b) Zr I and Zr II lines at depth 100 μm. (c) Strongly reabsorbed Ag lines from the interior of the experimental coated particle. (d) Ag lines from back surface paint layer seen in absorption.

Referring to Fig. 8, $\Delta E = 3.60$ eV ($5p^3G_5$), 3.66 eV ($5p^2P_{1/2}$), 5.08 eV ($4s^1P_{1/2}$) and 6.04 eV ($5d^2D_{3/2}$) respectively. Criterion (7) is therefore easiest to satisfy for the Ag/Zr density ratio, $n_e > 0.78 \times 10^{22}$ m^{-3} and hardest for the T_e measurement, $n_e > 3.5 \times 10^{22}$ m^{-3}.

To check whether inequality (7) was satisfied, the electron density was found from line widths. These were dominated by electron impact (Stark) broadening for the LIBS plasma studied:

$$n_e = \frac{\Delta\lambda}{w} 10^{23} m^{-3} \tag{8}$$

where $\Delta\lambda$ is the line width (FWHM) corrected for instrument broadening and w the stark broadening parameter (usually quoted for $n_e = 10^{23}\ m^{-3}$). These parameters have been calculated [35] for the resonance doublet of neutral silver (328.07 nm and 338.29 nm) and also measured [36] for the non-resonance doublet of 520.91 nm and 546.55 nm. Average values of $n_e = 6 \times 10^{23}\ m^{-3}$ were found for the conditions of interest implying relation (7) should be satisfied for all the measurements reported here. This density was also sufficiently low to justify the assumption that particle densities are predominantly of neutral species (see Eq. (5)).

In addition to satisfying Eq. (7) it is necessary to evaluate the implications of doing measurements on a highly transient and inhomogeneous plasma [33]. The advantage of working with neutral lines is that relevant relaxation times are much shorter than the time required to approach a Saha equilibrium between ionised and neutral species.

From Eq. (18) of Ref. [33] we can estimate the relaxation time from the excitation cross-section of the resonance transition of Ag I as $\tau_R \approx 0.04$ ns. This is sufficiently short compared with the time of ≈ 30 ns over which the bulk of the radiation is emitted that the plasma can be assumed to be quasi-stationary. With an estimate of an atom diffusion length from Eq. (20) of Ref. [33] as $D \approx 0.4$ cm^{2}s^{-1}, the diffusion length over τ_R is $\lambda \approx 0.04$ μm. This is considerably less than typical plasma dimensions of the order of 1 mm. Overall, therefore, LTE should be a reasonable assumption for the temperature and density measurements reported here.

We could measure intensity ratios down to 10^{-4} for the Ag I to Si I lines and about 5×10^{-2} for the Ag I to Zr I lines (higher due to line overlap). This implies estimates of density ratios down to 0.037% for n_{Ag}/n_{Si} and 0.026% for n_{Ag}/n_{Zr} (from Fig. 12). These limits should be completely adequate for studies with uranium plasmas.

5. Conclusions

We have experimentally found that femto-LIBS can achieve good surface spatial resolution and good depth resolution for studies of silver in experimental coated particles. We have detected and profiled

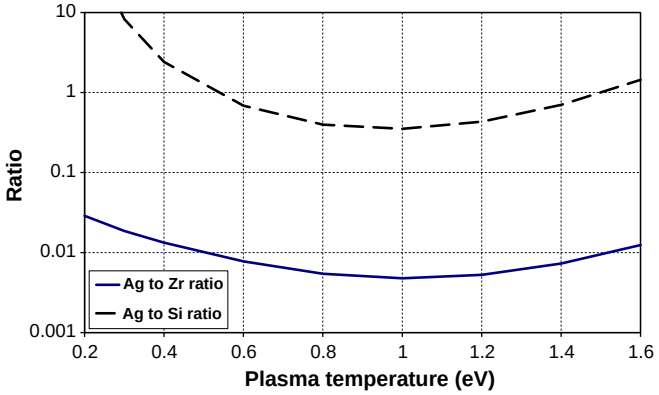

Fig. 12. Ratio of density of neutral silver to neutral silicon or zirconium for unit line intensity ratios.

Please cite this article as: D.E. Roberts, et al., Femtosecond laser induced breakdown spectroscopy of silver within surrogate high temperature gas reactor fuel coated particles, Spectrochim. Acta B (2010), doi:10.1016/j.sab.2010.09.001

silver with a depth resolution of approximately 1 μm, through a diameter of larger than 500 μm. We have shown that we could measure density ratios down to 0.037% for n_{Ag}/n_{Si} and 0.026% for n_{Ag}/n_{Zr}. This detection sensitivity should be sufficiently good that there should not be a major problem in investigating the loss of radioactive silver from actual high temperature gas reactor fuel kernels containing enriched uranium (with expected 0.6% silver content). One problem with femto-LIBS is that good depth resolution comes at the expense of good signal to noise ratios of LIBS signals, especially important when producing depth profile information through 500 μm depth. One potential way of improving this in future work is to use double-pulse LIBS [18–22]. In addition, further future work involves the detection of other impurities of concern to the nuclear fuel safety, for example caesium and strontium.

References

[1] K. Kugeler, R. Schulten, Hochtemperatur-Reaktortechnik, Springer, Berlin, Germany, 1989.
[2] Y. Katoh, N. Hashimoto, S. Kondo, L.L. Snead, A. Kohyama, Microstructural development in cubic silicon carbide during irradiation at elevated temperatures, J. Nucl. Mat. 351 (2006) 228–240.
[3] Y. Muto, S. Ishiyama, S. Shiozawa, Study of fission product release, plate-out and maintenance in helium turbomachinery, Proceedings of the IAEA Technical Committee Meeting on Gas Turbine Power Conversion Systems for Modular HTGRs (IAEA-TECDOC-1238), Palo Alto, Calif, USA, 2000, pp. 114–137.
[4] K. Verfondern, J. Sumita, S. Ueta, K. Sawa, Modeling of fuel performance and metallic fission product release behavior during HTTR normal operating conditions, Nucl. Eng. Des. 210 (2001) 225–238.
[5] K. Sawa, S. Suzuki, S. Shiozawa, Safety criteria and quality control of HTTR fuel, Nucl. Eng. Des. 208 (2001) 305–313.
[6] D.A. Petti, J. Buongiorno, J.T. Maki, R.R. Hobbins, G.K. Miller, Key differences in the fabrication, irradiation and high temperature accident testing of US and German TRISO-coated particle fuel, and their implications on fuel performance, Nucl. Eng. Des. 222 (2003) 281–297.
[7] A.I. van Heek, N.B. Siccama, P.H. Wakker, Fission product transport in the primary system of a pebble bed high temperature reactor with direct cycle, IAEA TECDOC-1238, 2000, pp. 138–148.
[8] J.J. Van der Merwe, Development and validation of fission product release models and software at PBMR, IAEA TECDOC-HTR-2004, 2004, pp. 1–21.
[9] H.J. MacLean, R.G. Ballinger, Silver ion implantation and annealing in CVD Silicon Carbide: the effect of temperature on silver migration, Second Topical Meeting on High Temperature Reactors 2004 (HTR-2004), Beijing, China, B23, 2004, pp. 1–20.
[10] Zirconium oxide properties, http://www.accuratus.com/zirc.html
[11] J.K. Fink, Thermo-physical properties of uranium dioxide, J. Nucl. Mat. 279 (2000) 1–18.
[12] V.T. Gotovchikov, V.A. Seredenko, V.V. Shatalov, V.N. Kaplenkov, A.S. Shulgin, V.K. Saranchin, M.A. Borik, C.W. Forsberg, Melted and Granulated Depleted Uranium Dioxide for Use in Containers for Spent Nuclear Fuel, IHLRWM 2006, Las Vegas, NV, April 30–May 4, 2006.
[13] US Department of Energy Report, 10 CFR Part 835, Occupational radiation protection, (1999) 425-460. See also www.sc.doe.gov/SC-80/sc-83/docs/835.pdf.
[14] D. Bodansky, Nuclear Energy: Principles, Practices and Prospects, Springer, New York, 2004 see also www.wise-uranium.org.
[15] Y. Duan, S.T. Scherrer, S.P. Koirala, C. Wang, C.B. Winstead, Uranium emission spectra with a low power microwave plasma source, Anal. Chim. Acta 532 (2005) 47–54.
[16] P. Fichet, P. Mauchien, C. Moulin, Determination of impurities in uranium and plutonium dioxides by laser-induced breakdown spectroscopy, Appl. Spectrosc. 53 (9) (1999) 1111–1117.
[17] D.E. Roberts, A. du Plessis, L.R. Botha, Femtosecond laser ablation of silver foil with single and double pulses, Appl. Surf. Sci. 256 (2010) 1784–1792.
[18] A. Semerok, C. Dutouquet, Ultrashort double pulse laser ablation of metals, Thin Solid Films 453–545 (2004) 501–505.
[19] V.I. Babushok, F.C. DeLucia Jr., J.L. Gottfried, C.A. Munson, A.W. Miziolek, Review: double pulse laser ablation and plasma: laser induced breakdown spectroscopy signal enhancement, Spectrochim. Acta B 61 (2006) 999–1014.
[20] S. Noël, J. Hermann, Reducing nanoparticles in metal ablation plumes produced by two delayed short laser pulses, Appl. Phys. Lett. 94 (2009) 053120.
[21] T. Donnelly, J.G. Lunney, S. Amuroso, R. Bruzzese, X. Wang, X. Ni, Double pulse ultrafast laser ablation of nickel in vacuum, J. Appl. Phys. 106 (2009) 013304.
[22] V. Pinon, D. Anglos, Optical emission studies of plasma induced by single and double femtosecond laser pulses, Spectrochim. Acta B 64 (2009) 950–960.
[23] B.N. Chichkov, C. Momma, S. Nolte, F. von Alvensleben, A. Tünnermann, Femtosecond, picosecond and nanosecond laser ablation of solids, Appl. Phys. A 63 (1996) 109–115.
[24] S. Nolte, C. Momma, H. Jacobs, A. Tünnermann, B.N. Chichkov, B. Wellegehausen, H. Welling, Ablation of metals by ultrashort laser pulses, J. Opt. Soc. Am. B14 (10) (1997) 2716–2722.
[25] P.W. Milonni, J.H. Eberly, Lasers, John Wiley and sons, New York, 1988.
[26] A. Ciucci, M. Corsi, V. Palleschi, S. Rastelli, A. Salvetti, E. Tognoni, New procedure for quantitative elemental analysis by laser-induced plasma spectroscopy, Appl. Spectrosc. 53 (1999) 960–964.
[27] E. Tognoni, G. Cristoforetti, S. Legnaioli, V. Palleschi, Calibration-free laser-induced breakdown spectroscopy: state of the art, Spectrochim. Acta B 65 (2010) 1–14.
[28] J.C. Pickering, V. Zilio, New accurate data for the spectrum of neutral silver, Eur. Phys. J. 13 (2001) 181–185.
[29] Y. Ralchenko, A.E. Kramida, J. Reader, and NIST ASD team (2008). NIST Atomic Spectra Database (version 3.1.5), [online]. Available: http://physics.nist.gov/asd3 [2010, February 16]. National Institute of Standards and Technology, Gaithersburg, MD.
[30] A.W. Irwin, Polynomial partition function approximations of 344 atomic and molecular species, Astrophys. J. Suppl. Ser. 45 (1981) 621–633.
[31] H.R. Griem, Plasma Spectroscopy, McGraw-Hill Inc., New York, 1964.
[32] C. Aragon, J. Bengoechea, J.A. Aguilera, Influence of optical depth on the line emission from laser-induced plasmas, Spectrochim. Acta B 56 (2001) 619–628.
[33] G. Cristoforetti, A. De Giacomo, M. Dell'Aglio, S. Legnaioli, E. Tognoni, V. Palleschi, N. Omenetto, Local thermodynamic equilibrium in laser-induced breakdown spectroscopy: beyond the McWhirter criterion, Spectrochim. Acta B 65 (2010) 86–95.
[34] R.W.P. McWhirter, in: R.H. Huddlestone, S.L. Leonard (Eds.), Plasma Diagnostic Techniques, Academic Press, New York, 1965, pp. 201–264, Chapter 5.
[35] M.S. Dimitrijevic, S. Sahal-Brechot, Stark broadening of Ag I spectral lines, Atom. Dat. Nucl. Tab. 85 (2003) 269–290.
[36] S. Djenize, A. Sreckovic, S. Bukvic, The first measured Ag I, Ag II and Ag III Stark broadening parameters, Spectrochim. Acta B 60 (2005) 1552–1555.

Please cite this article as: D.E. Roberts, et al., Femtosecond laser induced breakdown spectroscopy of silver within surrogate high temperature gas reactor fuel coated particles, Spectrochim. Acta B (2010), doi:10.1016/j.sab.2010.09.001